Carbohydrate Polymers 278 (2022) 118926

Contents lists available at ScienceDirect

Carbohydrate Polymers

journal homepage: www.elsevier.com/locate/carbpol

Hybrid PCL/chitosan-PEO nanofibrous scaffolds incorporated with *A. euchroma* extract for skin tissue engineering application

Fatemeh Asghari [a], Davood Rabiei Faradonbeh [b], Ziba Veisi Malekshahi [b], Houra Nekounam [a], Behnaz Ghaemi [a], Yaser Yousefpoor [c], Hossein Ghanbari [a], Reza Faridi-Majidi [a,*]

[a] Department of Medical Nanotechnology, School of Advanced Technologies in Medicine, Tehran University of Medical Sciences, Tehran, Iran
[b] Department of Medical Biotechnology, School of Advanced Technologies in Medicine, Tehran University of Medical Sciences, Tehran, Iran
[c] Research Center of Advanced Technologies in Medicine, Torbat Heydariyeh University of Medical Sciences, Torbat Heydariyeh, Iran

ARTICLE INFO

Keywords:
Biomaterials
Skin tissue engineering
Hybrid nanofibrous scaffolds
Electrospinning

ABSTRACT

Skin tissue engineering is an advanced method to repair and regenerate skin injuries. Recent research is focused on the development of scaffolds that are safe, bioactive, and cytocompatible. In this work, a new hybrid nanofibrous scaffold composed of polycaprolactone/chitosan-polyethylene oxide (PCL/Cs-PEO) incorporated with Arnebia euchroma (*A. euchroma)* extract were synthesized by the two-nozzle electrospinning method. Then the synthesized scaffold was characterized for morphology, sustainability, chemical structure and properties. Moreover, to verify their potential in the burn wound healing process, biodegradation rate, contact angle, swelling properties, water vapor permeability, mechanical properties, antibacterial activity and drug release profile were measured. Furthermore, cytotoxicity and biocompatibility tests were performed on human dermal fibroblasts cell line via XTT and LDH assay. It is shown that the scaffold improved and increased proliferation during in-vitro studies. Thus, results confirm the efficacy and potential of the hybrid nanofibrous scaffold for skin tissue engineering.

1. Introduction

Management of deep and large wounds is one of the most challenging medical complications (Okur, Karantas, Şenyiğit, Üstündağ Okur, & Siafaka, 2020). In order to develop an instant and efficient healing of skin injury, restoring barrier function and skin coverage is the initial step (Madni, Kousar, Naeem, & Wahid, 2021). Skin tissue engineering and regeneration are cost-effective and user-friendly methods for creating synthetic or engineered skin grafts which can be applied to heal acute and chronic skin wounds (Wei et al., 2021). A biocompatible, biodegradable, noninflammatory, and non-toxic biomaterial is vital for an effective skin regeneration and tissue engineering (Wei et al., 2021). According to the wound type, various types of dressings can be considered as wound dressing; however, they are mainly not designed on a functional basis (Rezvani Ghomi, Khalili, Nouri Khorasani, Esmaeely Neisiany, & Ramakrishna, 2019). Traditional wound dressings like gauze, bandages, and cotton wool are recently modified to support the wound area against microorganism contaminants (Boateng, Matthews, Stevens, & Eccleston, 2008; Goonoo & Bhaw-Luximon, 2020). Due to traditional wound dressings' adherence properties, detaching from the lesion area complained as a serious, painful complication. This type of mechanical wound dressings is applied only for uninfected wounds with moderate exudate conditions (Lei et al., 2019; Rezvani Ghomi et al., 2019). On the other hand, functional wound dressings such as hydrogels and hydrocolloids have been developed to overcome the limitations and disadvantages of traditional ones (Rezvani Ghomi et al., 2019). Functional wound dressing can contain specific therapeutic agents or bioactive materials like antimicrobial agents, growth factors, and enzymes to protect wounds from infection, promote cell proliferation, enhance proteolytic function and eliminate dead tissues (Dhivya, Padma, & Santhini, 2015).

Researchers have recently developed functional scaffolds for skin regeneration and tissue engineering. These scaffolds act as a physical barrier against microorganism infection and support the proliferation of dermal fibroblast and keratinocyte cells leading to skin remodeling. Moreover, an appropriate scaffold must prevent scar formation in the wound area (Zhong, Zhang, & Lim, 2010). The various properties of biomaterial scaffolds, e.g., mechanical strength, surface properties,

* Corresponding author.
E-mail address: refaridi@sina.tums.ac.ir (R. Faridi-Majidi).

https://doi.org/10.1016/j.carbpol.2021.118926
Received 4 August 2021; Received in revised form 26 October 2021; Accepted 19 November 2021
Available online 26 November 2021

biodegradation, and porosity, play a critical role in cell interactions (Qian, Zhang, Zheng, Song, & Zhao, 2014). Fabricating such functional scaffolds can be performed through different techniques, including electrospinning, phase separation, freeze-drying, self-assembly, and 3D bioprinting (Janarthanan & Noh, 2021; Lu, Li, & Chen, 2013). Producing scaffolds through this method require specific parameters and conditions to obtain special characteristic and topographies. Synthetic and natural biopolymers are the main biomaterials that provide promising biodegradation, biocompatibility, and bioactivity properties for skin tissue engineering applications (Kohane & Langer, 2008). Polymers like collagen, hyaluronic acid, and glycosaminoglycans of the extracellular matrix (ECM) can trigger cell attachment and control cell function (Sell et al., 2007). Cellulose, chitosan, and silk fibroin are also natural polymers that can be used for scaffold production to provide a desirable environment for cell growth and proliferation (Sell et al., 2007). However, there are some limitations in using natural polymers, including the possibility of contamination with the pathogens, difficulties of sterilization and purification process, and fast degradation rates (Dawson, Mapili, Erickson, Taqvi, & Roy, 2008; Ghasemi-Mobarakeh et al., 2015). To overcome these issues, synthetic polymers like polylactic acid (PLA), polycaprolactone (PCL), poly lactide-*co*-glycolide (PLGA), and polyurethane (PU) can be considered as ideal biomaterials owning appropriate physicochemical and mechanical properties in tissue engineering (Wei et al., 2021). Electrospun nanofibrous scaffolds as a wound dressing can stop fluid and protein loss, absorb exceeded exudates from the wound area, prevent microbial contamination, and conduct cells to proliferate and grow (Ramalingam & Ramakrishna, 2017). In addition, nutrient, oxygen, and waste diffusion are accomplished via nanofiber interconnected porous networks (Loh & Choong, 2013). Hybrid scaffolds made of both synthetic and natural biopolymers showed the durability and strength of synthetic polymers accompanied by the bioactivity and biocompatibility of natural polymers (Sionkowska, 2003). Moreover, natural biopolymers can improve the hydrophilicity of synthetic polymers to promote further cell adhesion and proliferation on the scaffolds (Goonoo et al., 2017; Goonoo & Bhaw-Luximon, 2020; Goonoo, Bhaw-Luximon, Jonas, Jhurry, & Schönherr, 2017). A recent study showed the potential of fabricated nanofibrous membranes by electrospinning poly(ε-caprolactone)(PCL) and quaternized chitosan-*graft*-polyaniline (QCSP) with antibacterial, electroactivity, and also anti-oxidant activity for wound dressing application (He, Liang, Shi, & Guo, 2020). Also, the mixture of chitosan oligosaccharides and quercetin/Rutin (Qe/Ru) with PCL polymer provided a new hydrophilic electrospun nanofiber membrane with antioxidant and bacteriostatic properties for wound healing applications (Zhou et al., 2021). One of the strategies in fabricating nanofibrous scaffolds for skin tissue engineering is the loading of antibacterial, antimicrobial, and antioxidant agents in the nanofibers. This materials can be included metallic nanoparticles, carbon based-composite and herbal medicine (Vijayakumar, Samal, Mohanty, & Nayak, 2019). Incorporating these components into nanofibrous scaffolds demonstrate several pharmacological effects which can react against inflammation and microorganism infection in wounds area (Ramalingam & Ramakrishna, 2017). Herbal extracts possess various biological constituent and chemical molecules which can act as an effective treatment for different wound healing related pathways and mechanism like expression and regulation of related genes and proteins leading to cell migration, adhesion and proliferation (Okur et al., 2020). Moreover, herbal medicine can promote wound healing process via various multifunctional effect like anti-inflammatory, antibacterial, antioxidative (Budovsky, Yarmolinsky, & Ben-Shabat, 2015). For example, In a study have recently conducted by Yin et al., they have developed a new self-made free surface electrospinning (FSE) device to fabricate polycaprolactone/chitosan/*aloe vera* in order to the antibacterial wound dressing with a good antibacterial activity against bacteria (Yin & Xu, 2020).

Arnebia Euchroma (*A. euchroma*) is a family of Boraginaceae that traditionally was used to treat skin wounds infections (Lu, Jiang, & Chen, 2004). The principal representative pharmacological constituents in the root of *A. euchroma* are naphthoquinone that mostly consists of alkannin and shikonin, and their derivatives (Kumar et al., 2021). Many studies have confirmed that naphthoquinones and their derivatives have numerous biological activities like anti-inflammatory, wound healing ability, radical scavenging activity, antibacterial and antifungal effects (Kumar et al., 2021; Papageorgiou, Assimopoulou, Couladouros, Hepworth, & Nicolaou, 1999; Xu et al., 2021; Zhishu, Min, Lin, & Lianquan, 2000). Since various secondary metabolites of herbal extracts can act as synergistic or additive wound healing effects related to *A. euchroma* root, using the complex molecules of the extract and its derivatives can be considered a suitable biomaterial for wound healing application (Cao et al., 2020).

Different wound care product has been listed in Table 1 which some of them are based on nanofibrous scaffolds. Recent studies confirmed that nanofibrous scaffolds play an essential role in designing and developing functional wound healing products (Ramalingam & Ramakrishna, 2017). As mentioned before, an ideal wound dressing must be antibacterial, biocompatible, absorb excess exudates, easy to remove, and cost-effective (Ramalingam & Ramakrishna, 2017). Nanofibrous scaffolds as a wound dressing can possess these properties and are a good candidate for wound healing.

In this study, we have developed a new type of advanced functional nanofibrous scaffolds, a hybrid scaffold of Polycaprolactone (PCL) and chitosan/polyethylene oxide (Cs/PEO) hybrid nanofibrous scaffolds synthesizing with two-nozzle electrospinning method. *A. euchroma* was incorporated in PCL solution due to its hydrophobic nature. Obtained nanofibrous scaffold were assessed for their chemical composition and morphology followed by scanning electron microscopy (SEM), FTIR, tensile mechanical testing, contact angle measurements, swelling property, water vapor permeability, in vitro biodegradation assays, drug release profile, and antibacterial activity. Then, a cytotoxicity study was performed on human dermal fibroblasts (HDF) cell line, followed by investigating its potential in burn wound healing and treatment applications. The results demonstrated that the prepared nanofibrous

Table 1
Different wound care product.

Product	Structure	Function	References
Integra™	A porous matrix of cross-linked bovine tendon collagen and glycosaminoglycan	Provide a wound matrix for cellular proliferation and growth	(Ramalingam & Ramakrishna, 2017)
Apligraf	One layer of differentiated keratinocytes and another layer of fibroblasts in a collagen matrix	Treatment of diabetic foot ulcer and venous leg ulcer	(Ramalingam & Ramakrishna, 2017)
DermaFuse™	A bioactive borate glass nanofibrous scaffold	wound healing	(Rahaman et al., 2011)
TransCyte	Human dermal tissue combined with a synthetic epidermal layer	Treatment of burns	(Ramalingam & Ramakrishna, 2017)
Tegaderm™	Thin polyurethane membrane coated with a layer of an acrylic adhesive	Transparent dressing for wound care	(Ramalingam & Ramakrishna, 2017)
Biobrane™	Composition of nylon mesh, silicone and collagen	One type of artificial skin for skin substitute	(Ramalingam & Ramakrishna, 2017)
Dermagraft-TC	fibroblast-derived temporary skin substitute	Wound covering for partial-thickness burns	(Truong, Kowal-Vern, Latenser, Wiley, & Walter, 2005)
ChitoFlex	Chitosan dressing	Hemostatic and antibacterial dressing	(Devlin, Kircher, Kozen, Littlejohn, & Johnson, 2011)

scaffolds have an excellent prospect in tissue engineering and regenerative medicine, which may notably improve the wound healing process.

2. Materials and methods

2.1. Materials

Polycaprolactone (PCL, MW = 80 KD), chitosan (CS, MW = 100 KD), and polyethylene oxide (PEO, MW = 900 KD, Acros Organics Co) was purchased from Easter Group (Dong Chen) Co., Ltd., China. Glacial acetic acid, methanol, and chloroform were purchased from Merck Co., Germany. Fetal Bovine Serum (FBS) and DMEM-high glucose media were all purchased from Gibco (USA). XTT Kit was purchased from Roche (Switzerland). Human Dermal Fibroblast cells, HDF (IBRC, C10506), were supplied by the Iranian Biological Resource Center.

2.2. Methods

2.2.1. Nanofibrous scaffold synthesis by two-nozzle electrospinning

To prepare electrospinning polymer solution, Chitosan (Cs) and Polyethylen oxide (PEO) were dissolved separately in glacial acetic acid 80.0% (*v*/v) at 55 °C under magnetic stirrer overnight to form a 2.5% *w/v* polymer solution. Then to prepare Cs/PEO solution, Cs and PEO solutions were blended together with ration of 8:2 (Cs:PEO) (Ketabchi et al., 2020). Also, Polycaprolactone (PCL) solutions were prepared in chloroform: methanol (7:3 *v*/v) under gentle stirring overnight at room temperature to make 9.0% *w/v* polymer solution.

2.2.2. Preparation of PCL/Cs-PEO/A. euchroma extract nanofibers

We used a two-nozzle electrospinning tool for electrospinning processes (Electroris, FNM, Tehran, Iran). The optimizing condition of two-nozzle electrospinning was carried out in a similar condition for two polymer solutions. Polymeric solutions were transferred into a 5 mL syringe with a metallic blunt-ended 18G stainless steel needle as a nozzle connected to a high voltage power supply. A voltage of 22 kV between the needle and the collector was applied with a rotation speed of 300 rpm and a 1 mm/h injection rate at ambient temperature.

Four concentrations of Arnebia Euchroma (*A. euchroma)* extract were blended in a 9.0% PCL solution. The PCL solution was stirred at room temperature, and the extract was later added with 10 *w/v*%, 15 w/v%, 20 w/v%, and 25 w/v% concentrations. After stirring for 3 h., the solution was electrospunned in two-nozzle electrospinning to obtain *A. euchroma* containing PCL nanofibers. Before this, *A. euchroma* extract was extracted using a maceration method that was then purified and dried to prepare for electrospinning. To fabricate two-layered electrospun membranes containing medicinal plant extract, the process was carried out by electrospinning of PCL-based solutions with various extract concentrations. One layer was *A. euchroma* containing PCL nanofiber, and the other layer was Cs-PEO nanofiber which was synthesized by two-nozzle electrospinning. The nanofibrous mats were then dried for 24 h at room temperature for more characterizations.

2.2.3. Scanning electron microscopy

Scanning Electron Microscopy (SEM, XL 30, Philips, USA) was used to characterize and investigate the surface morphology, diameter of nanofibers, and micro-and nanostructure of the scaffolds. The images were obtained using an accelerating voltage of 25.0 kV, and a small piece of each sample was sputter-coated with gold before observation. Then electronic micrographs were assessed via ImageJ software (Java 1.8.0_172, NIH) to compute the average diameter of approximately 50 nanofibers.

2.2.4. Fourier-transform infrared spectroscopy (FTIR)

The nanofiber's IR spectrum was obtained from the FTIR spectrometer located in the mid-IR region between 400 and 4000 cm^{-1}. Transition energies related to changes in vibrational energy state for numerous functional groups can indicate the appearance of an absorption band in this region, which can be used to determine the existence of specific functional groups within the structure. This characterization was used to investigate the structural changes due to the addition of medicinal plant extract (Mohamed, Jaafar, Ismail, Othman, & Rahman, 2017).

2.2.5. Contact angle measurement

To determine the degree of hydrophilicity of the surface, contact angle measurement was used. As defined in the literature, a hydrophilic surface possesses a contact angle of less than 90°, and a hydrophobic surface has a contact angle of more than 90° (Gittens et al., 2014).

2.2.6. Mechanical properties

The mechanical properties of the polymeric nanofibers scaffold were assessed through a uniaxial tensile test using Instron 5566. The nanofiber strips (1 mm × 3 mm) were located in a window frame and mounted on the grip of the tensile instrument. Before the start of the test, the vertical ribs of the frame were cut. The strain rate for stretching strips was set at 1 $mm.min^{-1}$. Scaffolds were stretched until failure, and then stress-strain curves were recorded. Young's Modulus (E) was computed from the slope of stress-strain curves in the range of 5–10% strain.

2.2.7. Swelling study

The swelling ratio of the polymeric nanofibrous scaffolds was carried out after immersing and incubation them in PBS for 1, 6, 12, and 24 h at 37 °C. The weights of the swollen nanofibers were calculated after discarding the excess PBS from the surface of the scaffolds using filter paper. Then the swelling ratio of the nanofibrous scaffolds was evaluated by the following equation:

$$\%\text{Swelling ratio} = (W_s{}^{-}W_d/W_d)*100$$

where W_s and W_d represent the weights after swelling and the dry weight of nanofibers respectively.

2.2.8. Water vapor permeability (WVP)

Water vapor permeability was evaluated based on the BS 7209 method. Forty milliliter of water was firstly added to a dish with an internal diameter of 83 mm and the area of the dish was 54.1 cm^2. The dish with nanofibrous scaffolds was placed on a turntable, and the primary weight of the assembly was measured (Chen, Tu Fan, Sarkar, & Bal, 2011).

2.2.9. Biodegradation

All nanofibers were cut with a diameter of 15 mm, then accurately weighed and immersed in PBS containing 0.1 M lysozyme (Sigma Aldrich). Scaffolds were agitated in a shaker incubator at 37 °C with 100 rpm for 28 days. After distinct time points, nanofibers were removed and washed with distilled water three times, then dried in an oven for 48 h. Three samples were weighted at each distinguished interval to assess the weight loss of polymeric nanofiber scaffolds. The weight loss of nanofibers was computed with the following equation:

$$\%\text{Weight loss} = (W_i{}^{-}W_d/W_i)*100$$

W_i and W_d represent the initial dry weight and the dry weight after soaking for determined intervals, respectively.

2.2.10. Sustainability

To estimate nanofibers' stability in an aqueous medium, specified sizes of nanofiber scaffolds were immersed into phosphate buffer saline (PBS, pH = 7.4) at 37 °C for 1 day, and then the structural and morphological changes were evaluated via SEM imaging after drying in room temperature.

2.2.11. Cytotoxicity assays

Cytotoxicity assay of nanofiber scaffolds was evaluated by XTT assay (Roche, Switzerland) and Lactate dehydrogenase (LDH) assay. The nanofibers were placed into 48- well plates in self-seal. Then Samples were located in a Gamma beam 651PT irradiation chamber, and Gamma-irradiation sterilization was obtained at a dose of 25 kGy at room temperature. Before the sterilization process, all samples were Fixed using medical-grade O-rings (*C. Otto* Gehrckens GmbH & Co, Germany) to avoid any movement and ensure appropriate cell seeding on top of the nanofiber scaffolds. Human dermal fibroblast (HDF) cell line was purchased from the Iranian Biological Resource Center (IBRC) and pre-cultured in high glucose Dulbecco's Modified Eagle Medium (DMEM, Gibco), supplemented with 10% Fetal Bovine Serum (FBS, Gibco), and 1% antibiotic (penicillin-streptomycin, Gibco). Cell seeding was performed in 48-well tissue culture plates at a cell density of 1×10^4 cells per well for 1- and 3-day experiments. In brief, media of each well was transferred to another plate to react with the XTT reaction mixture. The light-protected plate was incubated for the next 3 h. The absorbance was read at 450 nm for XTT assay using a plate reader (Cytation 5, Biotek). The results of this assay were normalized to tissue culture plastic (TCP) controls.

The cytotoxicity effect of nanofibrous scaffolds on human dermal fibroblasts was assessed by the LDH Cytotoxicity kit (Roche Diagnostics, Germany) according to the manufacturer's protocol. Briefly, HDF cells ($n = 1 \times 10^4$) were seeded on the nanofibrous scaffolds in plates and incubated in a 37° C incubator with 90% humidity and 5% CO2. DMEM media without phenol red and 1% FBS was used because of the interference of phenol red and FBS with LDH adsorption. After the different incubation times, the cell culture media were extracted, and 100 μl DMEM media was added to each well. Subsequently, the lysing solution was added and incubated for 15 min to attain complete cell lysing. Finally, the cell culture media was moved entirely to other plates and mixed well with the LDH reaction mixture. Absorbance was measured at 490 nm after 30 min in dark conditions at room temperature.

2.2.12. Cell attachment and morphology

To assess cell attachment and configurations on the synthesized nanofiber scaffolds, SEM imaging was used. In brief, HDF cells were seeded on all types of scaffolds, and after five days, the seeded cells were fixed with 2.5 *v*/v% glutaraldehyde and 4 *w*/*v*% paraformaldehyde. Next step was ethanol treatment 30%, 50%, 70%, 90%, and 100% were performed, each for 5 min. After treatment with ethanol, all samples were sputter-coated with gold, and SEM was carried out to imaging cell attachment and morphology.

2.2.13. In-vitro drug release study

The release profile of *A. euchroma* from nanofiber scaffolds were investigated in phosphate buffer saline (PBS), methanol 10 *v*/v%, and tween 80 0.5 v/v% (Han, Zhang, Zhu, & Branford-White, 2009; Lou, Wu, Lee, Chen, & Lin, 2017; Taepaiboon, Rungsardthong, & Supaphol, 2007). To obtain a calibration curve, specific concentration of *A. euchroma* in PBS was prepared and shacked to homogenize the solution. Then the solution was scanned for finding the λ_{max} by using a UV–Vis spectrophotometer (UV–Visible (SHIMADZU)). To study the drug release profile, the pieces of nanofibers with a specific size (2.5 × 2.5 cm) were precisely weighted and placed into 10 ml phosphate buffer saline (PBS, pH = 7.4). Then the solutions were incubated under stirring 100 rpm at 37 °C for specific time intervals. Subsequently, aliquots of samples of about 3 ml were gathered from the release medium and replaced with fresh PBS at this time intervals: 0.5, 1, 2, 4, 6, 9,12, 24, 48, 72 and 96 h. Finally, the absorbance was studied using a UV–vis spectrophotometer at known λ_{max}. With the assist of the calibration curve, the percentage of drug releases was computed through changing absorbance to *A. euchroma* concentrations. Then the cumulative release was determined in specific time intervals.

2.2.14. Antibacterial activity

Dynamic contact assay was used to evaluate the antibacterial properties of fabricated nanofibrous scaffolds. Two Gram-negative and Gram-positive bacterial strains, *E. coli* (ATCC 25922) and *S. aureus* (ATCC 25923) were used at the concentration of 1×10^6 CFU/mL according to L. Zhou et al. study (Zhou et al., 2021). *E. coli* and *S. aureus* were first cultured in a shaker incubator under 200 rpm at 37 °C and then adjusted to an OD_{600} value of 0.5. To evaluate the dynamic contact assay, 15 mg of nanofibrous scaffolds were cut into small pieces and then incubated with 1 ml of the bacterial suspension up to 24 h under conditions of 200 rpm and 37 °C. After this time, 100 μL of the suspension was moved to a 96-well microplate, and the absorption of bacteria was measured at 600 nm. Each sample was repeated three times. The following equation computed the antibacterial activity:

$$\text{Antibacterial activity } (\%) = (1 - (S - SC)/C)^*100$$

where C, S, and SC are the control, sample, and sample control absorbance, respectively. According to our previous study (Asghari et al., 2021), the structure and surface morphologies of the bacteria on the nanofibrous scaffolds were imaged by SEM (Philips XL 30, Netherlands) after gold coating at a voltage of 25KV was applied to assess the bacteria's appropriate morphology.

2.2.15. Statistical analysis

The experiments were carried out with at least three repeats, and all results were expressed as means with standard deviation (M ± SD). One-way analysis of variance (ANOVA) was used, and $P < 0.05$ was considered the significance level for statistical analysis. All data were analyzed using the GraphPad Prism statistical software version 6.01 (GraphPad, CA, USA).

3. Results and discussion

3.1. Size and morphology of fabricated PCL/Cs-PEO/A. euchroma nanofiber

The structures, morphologies, and diameter of the fabricated Polycaprolactone/Chitosan-Poly ethylene Oxide (PCL/Cs-PEO) and Arnebia euchroma (*A. euchroma*) loaded PCL/Cs-PEO (10%, 15%, 20%, and 25%) nanofiber scaffolds were studied with SEM. The size distribution of nanofiber scaffolds has been shown in Fig. 1, which demonstrates consistent fiber size distribution across all samples despite the addition of extract. SEM images revealed PCL/Cs-PEO nanofiber without beads with the average diameters of 104 nm ± 36.5 (Fig. 1) that was analyzed by Image J software. It is worth noting that the diameter of PCL/Cs-PEO/*A. euchroma* 10%, 15%, 20%, and 25% nanofibers were 133 ± 29.7, 141 ± 38.6, 209 ± 83.3, and 396 ± 84.5 nm, respectively (Fig. 1). SEM images were also performed for PCL and Cs-PEO nanofibrous scaffold separately. The diameter of the PCL and Cs-PEO nanofibrous scaffold was measured 218 ± 36.3 and 112 ± 14.3, respectively. The size distribution of nanofiber scaffolds has been shown in Fig. 1, which demonstrates consistent fiber size distribution across all samples despite the addition of extract. The consistency in size distribution across samples plays a vital role in future scaffolds applications in regenerative medicine and tissue engineering. As can be seen in SEM micrographs of PCL/Cs-PEO/*A. euchroma*, nanofiber diameter was found to increase when the *A. euchroma* concentration was increased. A smaller fiber diameter possesses a larger surface area in nanoscale fibers, giving more space for cell attachment and better tensile properties that provide a substrate adequate for simulating the extracellular matrix (ECM) growth environment in vivo. Also, SEM images showed that the *A. euchroma* extract either embedded inside or dispersed on the polymeric nanofibers homogeneously, imparting a rough texture to the scaffolds. To better cell attachment and growth, increasing the surface roughness of a nanofibrous scaffold is desirable. Moreover, the porous

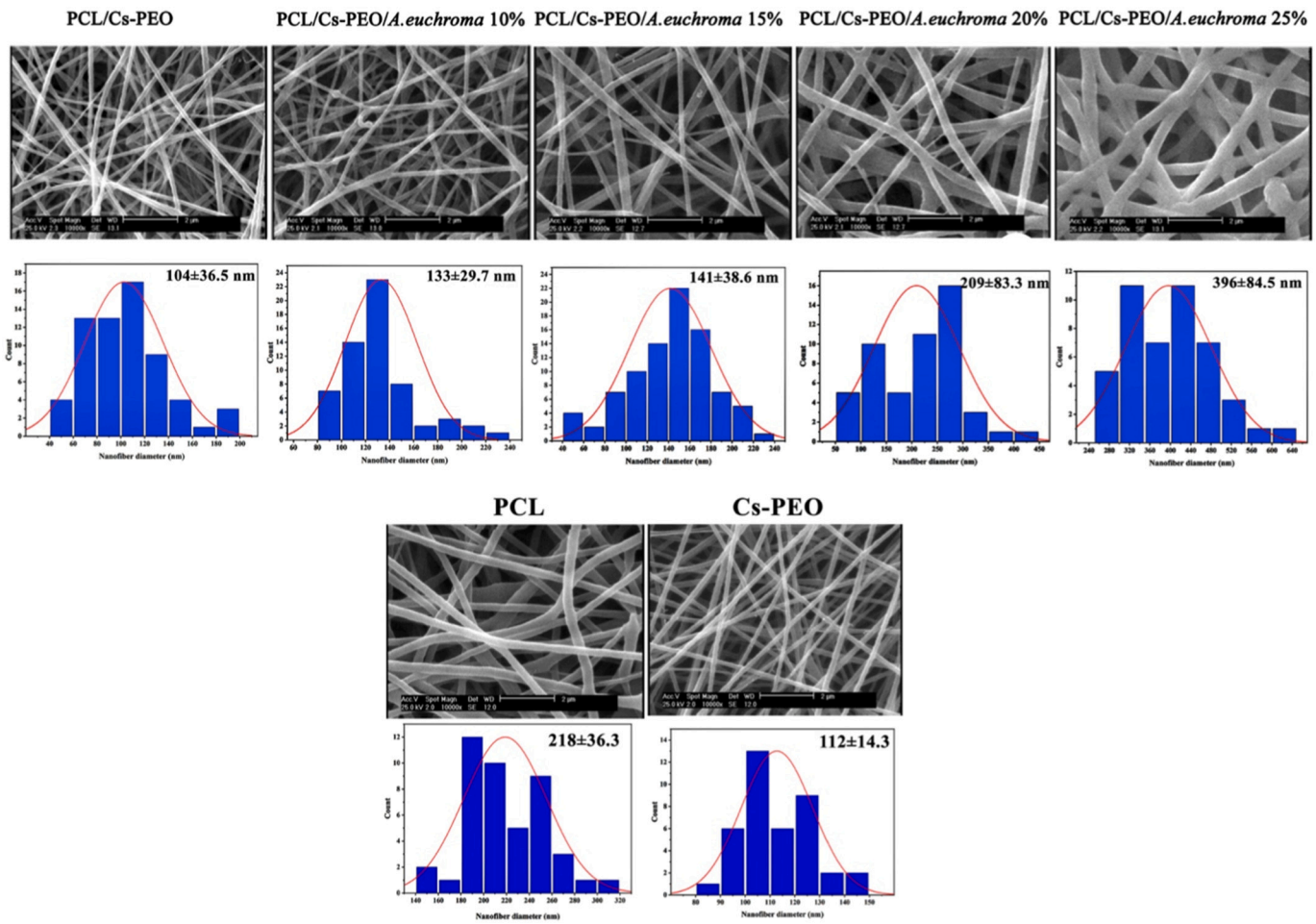

Fig. 1. SEM images of various nanofibrous scaffolds.

structure of electrospinning nanofibers scaffolds can supply sufficient cell growth space and be favorable to the transporting of nutrient material and growth factors. Nanofibrous scaffolds fabricated by two-nozzle electrospinning can mimic the extracellular matrix (ECM) to promote the adhesion of skin cells and can be used as a template for wound healing and skin tissue regeneration (Barnes, Sell, Boland, Simpson, & Bowlin, 2007; Gao et al., 2021). The two-layered electrospun membranes have been fabricated by natural polymer and synthetic polymer without any cross-linking method or using toxic solvents such as HFIP and TFA. Moreover, using natural biopolymers and synthetic polymers in the structure of nanofibers simultaneously can improve some properties of scaffolds like compositional and structural effects, mechanical strength, and synergistic effect of materials. Natural polymers have biocompatible and biodegradable natures. Chitosan is one of the natural biopolymers and is widely used for fabricating and designing nanofibrous scaffolds due to its cost-effectiveness, appropriate antibacterial properties, and acceptable biocompatibility and biodegradability. Besides, chitosan has been widely used as a promising natural biopolymer in tissue engineering applications for wound dressing (Fernandes Queiroz, Melo, Sabry, Sassaki, & Rocha, 2015; Islam, Shahruzzaman, Biswas, Sakib, & Rashid, 2020). Even though, the spinnability and reproducibility of chitosan solution to fabricate pure and stable nanofibers have remained a challenge. Blending of chitosan biopolymer with other polymers like Polyvinyl alcohol (PVA), Polyethene oxide (PEO), and collagen have been widely used to facilitate the chitosan electrospinning process to address this problem (Ketabchi et al., 2020). To fabricate Cs-PEO nanofibers, the spinning solutions are obtained by blending the two polymers solutions prepared separately in the same solvent. PEO has excellent spinnability and can affect the electrospinning process. Moreover, PEO polymer can interact with chitosan, which is desirable to chitosan electrospinning, and also, PEO is non-toxic (Abid et al., 2019). On the other hand, synthetic polymers have been used in tissue engineering applications due to their excellent physical and mechanical properties, appropriate biocompatibility, and good reproducibility (Akbarinejad, Ghoorchian, Kamalabadi, & Alizadeh, 2016). Polycaprolactone (PCL) is one of the most common synthetic polymers widely applied in tissue engineering applications due to its excellent mechanical strength and good biodegradability (Hiep & Lee, 2010). When PCL blends with natural biopolymer can improve the mechanical strength of natural biopolymer nanofibers (Chanda et al., 2018). Moreover, the blending of synthetic and natural polymeric nanofibers is able to mimic a desirable extracellular matrix for the growth of different cells. Results of some researches have confirmed that blending PCL with natural polymers can improve the proliferation rate of fibroblasts cells and also show a more normal morphology compared with PCL nanofibers (Gao et al., 2021).

3.2. Fourier-transform infrared spectroscopy (FTIR)

FTIR analysis was used to characterize functional groups in the nanofiber scaffolds to confirm the existence of the scaffold component and to distinguish any possible chemical modification or interaction between phases. The chemical structures of the Cs-PEO (Fig. 2a), PCL (Fig. 2b), PCL/Cs-PEO (Hild et al., 2015) (Fig. 2c), PCL/Cs-PEO/*A. euchroma* 10% (Fig. 2d), PCL/Cs-PEO/*A. euchroma* 15% (Fig. 2e), PCL/Cs-PEO/*A. euchroma* 20% (Fig. 2f), and PCL/Cs-PEO/*A. euchroma*

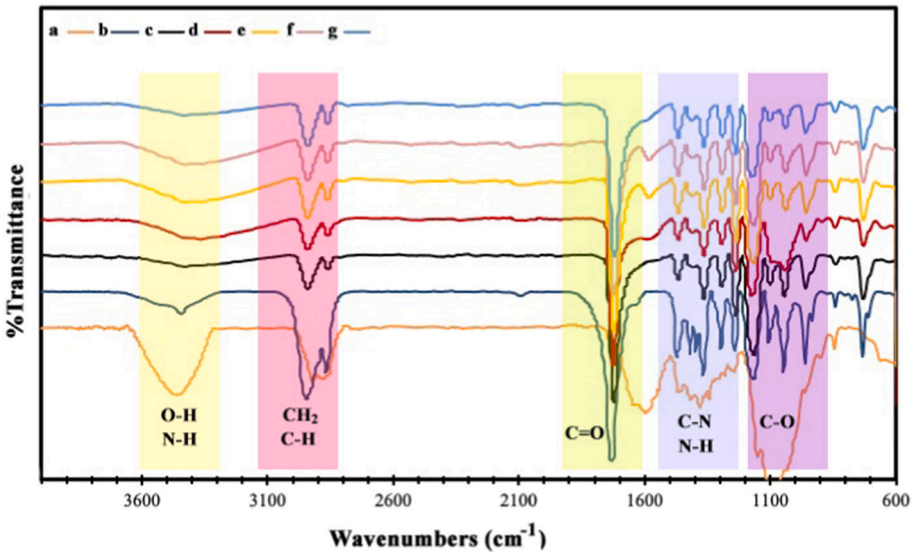

Fig. 2. FTIR spectra of PCL/Cs-PEO and PCL/Cs-PEO/*A. euchroma* nanofibers with different weight ratios of *A. euchroma*. a) Cs-PEO, b) PCL, c) PCL/Cs-PEO nanofibers, d) PCL/Cs-PEO/A.Echroma 10%, e) PCL/Cs-PEO/*A. euchroma* 15%, f) PCL/Cs-PEO/*A. euchroma* 20%, g) PCL/Cs-PEO/*A. euchroma* 25%.

25% (Fig. 2g) scaffolds were shown. The characteristic peaks of PCL at 2938, 2865, and 1724 cm^{-1} can be attributed to the asymmetric CH_2 stretching, symmetric CH_2 stretching, C═O stretching vibration, respectively. The peak at 1724 cm^{-1} is related to the C═O stretching vibration of the ester group. C—H stretching vibrations of PEO molecules were attributed to the peaks at around 2891 cm^{-1}. Also, stretching vibrations of C—O in PEO molecular chain has been shown in the peak at 1100 cm^{-1}. The peak at 3433, 2850, 1665, 1388 and 1070 cm^{-1} were ascribed to the amino groups N—H and O—H stretching vibrations, C—H stretching vibrations, C═O stretching of amide I, C—N stretching of amide III, and C—O stretching vibrations of Cs molecular chain respectively (Fernandes Queiroz et al., 2015; Song, Yu, Zhang, Yang, & Zhang, 2013; Vino, Ramasamy, Shanmugam, & Shanmugam, 2012). The strong peak viewed at 1555 cm^{-1} describes to the amine band in chitosan. Most of the characteristic peaks of the nanofiber scaffolds component were appeared in the spectra of the all composites. These results imply that PCL, Cs-PEO, and *A. euchroma* mixed properly with each other to make a homogeneous chemical structure after electrospinning process. Therefore, the above FTIR results confirmed that the nanofiber scaffolds consisted of PCL, Cs, and PEO (Pakravan, Heuzey, & Ajji, 2011; Wang et al., 2019).

3.3. Contact angle measurement

The wettability test was performed to prove the effect of extract on hydrophilicity or hydrophobicity of nanofiber scaffolds. Fig. 3 demonstrates the contact angle measurements results, which give some information on changes in surface properties due to the extract addition to the polymeric solution. The static contact angle of water droplets on PCL/Cs-PEO nanofibers was 55.5 ± 5°, which was different from *A. euchroma* loading PCL/Cs-PEO nanofibers. In addition, the static contact angle of water droplets on PCL/Cs-PEO/ *A. euchroma* 10%, PCL/Cs-PEO/*A. euchroma* 15%, PCL/Cs-PEO/*A. euchroma* 20%, and PCL/Cs-PEO/*A. euchroma* 25% nanofibers scaffolds were 63.9 ± 11°, 76.2 ± 2°, 97.2 ± 18°, and 107.0 ± 13°, respectively. It can be attributed to the hydrophobic nature of *A. euchroma* extract. Therefore, by increasing the extract ratio in PCL/Cs-PEO nanofibers, the hydrophilicity decreases. As reported in the literature, morphology, and surface chemistry

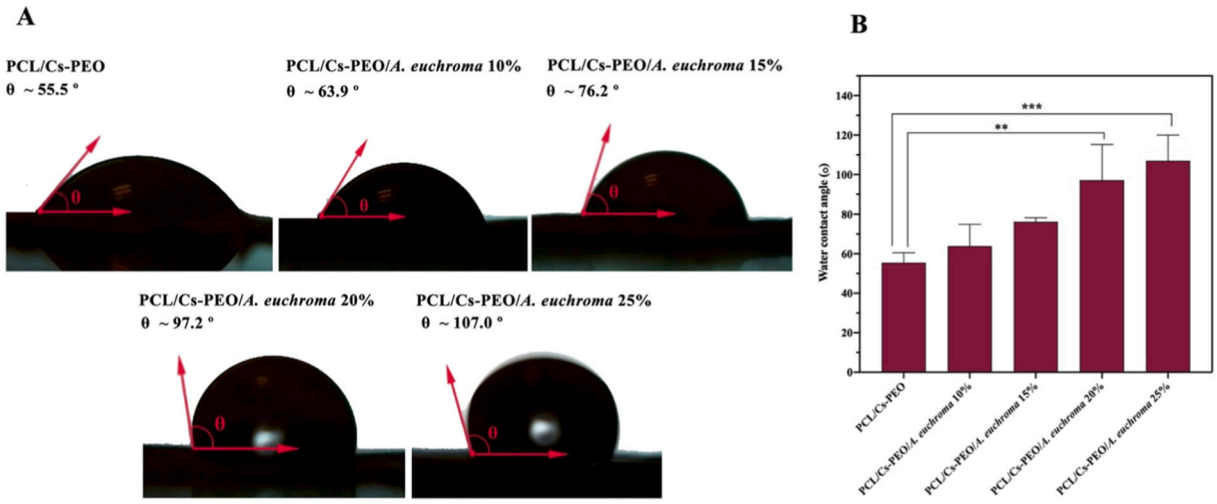

Fig. 3. Water contact angle measurement of different nanofibrous scaffolds (A). The histogram displays the water contact angle data measured with the various nanofibrous scaffolds. Also, Error bars show standard deviation (SD) (B). All samples were compared with PCL/Cs-PEO nanofiber **, referred to as $P \leq 0.0038$, *** and $P \leq 0.0008$.

modification are two main factors that can change wettability (Zhong et al., 2006). Moreover, topography and morphology can affect contact angle and chemical properties (Shalumon et al., 2011).

3.4. Mechanical properties of nanofibers

The mechanical behavior of PCL/Cs-PEO and PCL/Cs-PEO/*A. euchroma* nanofibers was reported in Table.2. Adequate mechanical properties are necessary for scaffolds to tolerate applied stresses in implantation application with sufficient flexibility. Mechanical properties such as the average ultimate tensile stress (σ_{UTS}), elongation rate, and Young's modulus (E) of the scaffolds were evaluated. According to the definitions, ultimate tensile stress (σ_{UTS}) describes the sample's first failure points, and Young's modulus (E) specifies as the slope of the linear region of the stress-strain curve below the yield stress. Results are shown in Table 1. The Young's modulus (E) of PCL/Cs-PEO, PCL/Cs-PEO/*A. euchroma* 10%, PCL/Cs-PEO/*A. euchroma* 15%, PCL/Cs-PEO/*A. euchroma* 20% and PCL/Cs-PEO/*A. euchroma* 25% nanofibers were 195.86 ± 8.23, 175.63 ± 2.05, 148.29 ± 78.09, 141.32 ± 16.50, and 133.28 ± 5.99 MPa, respectively. The average Young modulus (E) of the nanofibers scaffold decreased with adding *A. euchroma* and the ultimate tensile stress (σUTS) followed the same trend. According to the literature, the high value of mechanical properties such as strength and stiffness in nanofibrous scaffolds could be related to the formation of longer polymeric chains (Sonseca et al., 2014). On the other hand, the stiffness of PCL/Cs-PEO nanofibers can be attributed to the absolute temperature and the strand density of the polymer, which is in accord with prior studies related to the mechanical behavior (Feng, Xiong, Jiang, Liu, & Hou, 2016). The decreasing trends of Young Modulus (E) in PCL/Cs-PEO/*A. euchroma*, 15% nanofibers, compared to PCL/Cs-PEO/*A. euchroma* 20% and 25% didn't change considerably by increasing the amount of *A. euchroma*. The overall amount of Young Modulus in PCL/Cs-PEO/*A. euchroma* 20% and 25% nanofibers slightly decreased. It must be noted that this decrease in the two samples is not necessarily statistically different. It seems that the presence of *A. euchroma* between entangled polymeric chains, on the one hand, the mechanical behavior of PCL, Cs, and PEO polymers on the other hand, could facilitate the plastic deformation of nanofibrous scaffolds (Wang et al., 2018, 2019). Moreover, the strength of polymer expectedly decreases when a natural polymer is blended to a synthetic polymer (Lee et al., 2008). Since the human skin have tensile strength approximately of 2–16 MPa and Young's modulus about 6–40 GPa (Trinca, Westin, da Silva, & Moraes, 2017), all the nanofibrous scaffolds with and without medicinal plant can supply mechanically firm structures for skin tissue regeneration.

3.5. Swelling study

A swelling test was performed in PBS for 24 h. Fig. 4 demonstrates the swelling ratio of PCL/Cs-PEO and PCL/Cs-PEO containing 10, 15, 20, and 25% *A. euchroma* nanofibers after PBS treatment. The swelling capacity of nanofibrous scaffolds plays an important role in absorbing excess exudate in the wound area. Besides, the scaffolds with swelling properties can transfer cell nutrients and metabolites into the wound sites (Chanda et al., 2018). The swelling results demonstrated that the PCL/Cs-PEO, PCL/Cs-PEO/*A.euchroma* 10%, and PCL/Cs-PEO/*A. euchroma* 15% scaffolds improved swelling property PCL/Cs-PEO/*A. euchroma* 20% and PCL/Cs-PEO/*A.euchroma* 25% scaffold up to 24 h. The swelling capacity of the PCL/Cs-PEO, PCL/Cs-PEO/*A.euchroma* 10%, and PCL/Cs-PEO/*A.euchroma* 15%, PCL/Cs-PEO/*A.euchroma* 20%, and PCL/Cs-PEO/*A.euchroma* 25% scaffolds were 72 ± 6.71, 69 ± 10.6, 61 ± 18.74, 49 ± 8.84, and 24 ± 14.1 respectively until 24 h. The decreased swelling capacity of the PCL/Cs-PEO/*A.euchroma* 20% and PCL/Cs-PEO/*A.euchroma* 25% scaffolds can be attributed to the addition of hydrophobic *A.euchroma*. The swelling capacity of the nanofibrous scaffolds computed in this study was approximately similar to that of the scaffolds reported in the other literature (Chanda et al., 2018; Prasad, Shabeena, Vinod, Kumary, & Kumar, 2015).

Table 2
The mechanical test results of nanofibrous scaffolds.

Nanofibrous scaffolds	Young's modulus (E) MPa	Ultimate tensile stress (σ_{UTS}) MPa
PCL/Cs-PEO	195.86 ± 8.23	10.79 ± 0.75
PCL/Cs-PEO/*A. euchroma* 10%	175.63 ± 2.05	10.71 ± 1.28
PCL/Cs-PEO/*A. euchroma* 15%	148.29 ± 78.09	8.04 ± 3.17
PCL/Cs-PEO/*A. euchroma* 20%	141.32 ± 16.50	8.81 ± 1.91
PCL/Cs-PEO/*A. euchroma* 25%	133.28 ± 5.99	6.44 ± 0.18

3.6. Water vapor permeability

The results of WVP of the nanofibrous scaffolds have been shown in Table 3. A remarkable difference was not seen between the WVP of PCL/Cs-PEO and PCL/Cs-PEO incorporated with *A.euchroma*. Ideal moisture content plays a vital role in the wound healing process. The evaporative water on the wound sites is almost more significant than normal skin (Xu et al., 2016). It is proved that the cells need to moisture microenvironment to proliferation and good function. Therefore, they lose their vitality and function in dry conditions. Moreover, based on previous studies, the wound healing process can occur faster under wet conditions (Atiyeh, Ioannovich, Al-Amm, & El-Musa, 2002; Svensjö, Pomahac, Yao, Slama, & Eriksson, 2000; Winter, 1962). Hence, an appropriate wound dressing can be affected in adjusting water evaporation on the wound areas. Developing and designing a proper wound dressing is the main factor in maintaining optimal moisture in the wound areas (Xu et al., 2016). Exceedingly high water vapor permeability can cause dryness of a wound area; on the contrary, lower water vapor permeability can lead to the retention of wound exudates. Therefore, suitable WVP plays a critical role in providing a moist environment for proper wound healing. Based on R. Xu et al. study, an appropriate water vapor transmission rate can maintain the optimal moisture content for fibroblasts' cell proliferation and function (Xu et al., 2016).

3.7. Biodegradation study

Fig. 5B reveals nanofiber scaffolds' degradation and weight loss profiles in PBS solution containing lysozyme for up to 28 days. Lysozyme is the secondary granules of neutrophils; neutrophils are one of the first inflammatory cells that migrate to the wound sites and release some antimicrobial substances and proteases into the extracellular matrix (Takagi et al., 2017; Wilgus, Roy, & McDaniel, 2013). For this reason, the enzyme lysozyme was added to the PBS solution. This condition was simulated to mimic the in vivo. Due to the unknown physiological situation, there is no information about the accurate amount of dose of enzyme release. To have a suitable regeneration process, appropriate degradation behavior of scaffolds is necessary (Liu, Ma, & Gao, 2012). The in vitro degradation and weight loss properties of nanofibrous scaffolds were evaluated through measuring the weight of scaffolds. Due to PCL's hydrophobic nature and structure, the degradation rate of PCL is very slow and approximately 2–4 years (Cipitria, Skelton, Dargaville, Dalton, & Hutmacher, 2011). Owing to the enzymatic hydrolysis process, chitosan layer and *A. euchroma* was decomposed. It is noticed that all samples undergo a biodegradation process because of the weight loss in 28 days presented. During 28 days, the weight losses of nanofibrous scaffolds PCL/Cs-PEO, PCL/Cs-PEO/*A. euchroma* 10%, PCL/Cs-PEO/*A. euchroma* 15%, PCL/Cs-PEO/*A. euchroma* 20%, and PCL/Cs-PEO/*A. euchroma* 25% were calculated about 10 ± 0.83%, 22 ± 1.31%, 23 ± 0.44%, 26 ± 1.59% and 28 ± 1.73%, respectively. The biodegradation

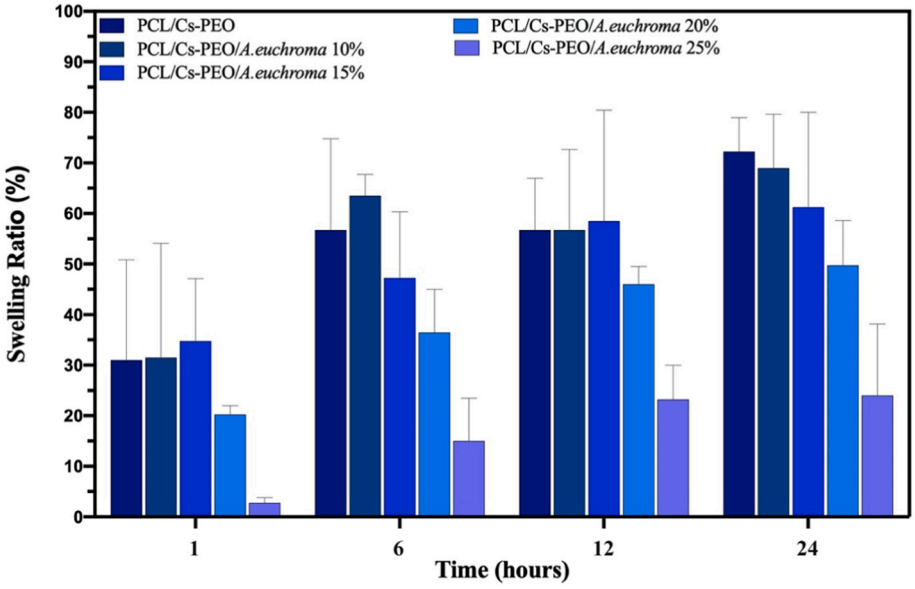

Fig. 4. Swelling ratio percentage of PCL/Cs-PEO nanofibers and PCL/Cs-PEO containing various concentration of *A.euchroma* in PBS (pH = 7.4, T = 37 °C) at different time intervals.

Table 3
Water vapor permeability (g/m^2/day) of various nanofibrous scaffolds were evaluated based on BS 7209.

Sample	Water vapor permeability (g/m^2/day)
PCL/Cs-PEO	21.44 ± 0.21
PCL/Cs-PEO/*A.euchroma* 10%	20.14 ± 0.01
PCL/Cs-PEO/*A.euchroma* 15%	20.94 ± 0.04
PCL/Cs-PEO/*A.euchroma* 20%	22.25 ± 0.12
PCL/Cs-PEO/*A.euchroma* 25%	22.83 ± 0.37

process did not attain a plateau phase and continuously increased over time. The fastest biodegradation rate occurred for a week. These results show that nanofibrous scaffolds' weight loss increased slightly when the concentration of *A. euchroma* increased. Scaffolds with 25% *A. euchroma* had a faster weight loss rate than that of other ones containing *A. euchroma*. It is noteworthy that the faster degradation rate of PCL/Cs-PEO/*A. euchroma* 25% nanofibrous scaffolds are probably related to the interaction between *A. euchroma* and the enzyme lysozyme. The results show by increasing the *A.euchroma* ratio in PCL/Cs-PEO nanofibers, the biodegradation rate increases. However, as mentioned in the literature, the degradation rate completely depended on the hydrophilicity nature, rates of crystallinity, molecular weight, polymer composition, and morphological structure (Zhou et al., 2015). Moreover, biodegradation of scaffolds under in-vivo situations plays a vital role in tissue engineering applications.

3.8. Sustainability test for nanofibers

SEM images of the nanofibrous scaffold, after 24-h immersing in PBS, have been shown in Fig. 5A. As can be seen in these images, when immersing happens, the diameter of nanofibrous scaffolds increases. For example, the diameter of nanofibers in PCL/Cs-PEO nanofibers increases from 104 ± 36.5 nm to 173 ± 28.1 nm same as the diameter of PCL/Cs-PEO/*A. euchroma* 10%, PCL/Cs-PEO/*A. euchroma* 15%, PCL/Cs-PEO/*A. euchroma* 20%, and PCL/Cs-PEO/*A. euchroma* 25% nanofibrous scaffolds enhanced 180 ± 55.7, 225 ± 38.8, 354 ± 45.5, and 441 ± 64.6 nm. The chitosan fibers lose their fibrous structure when contact with

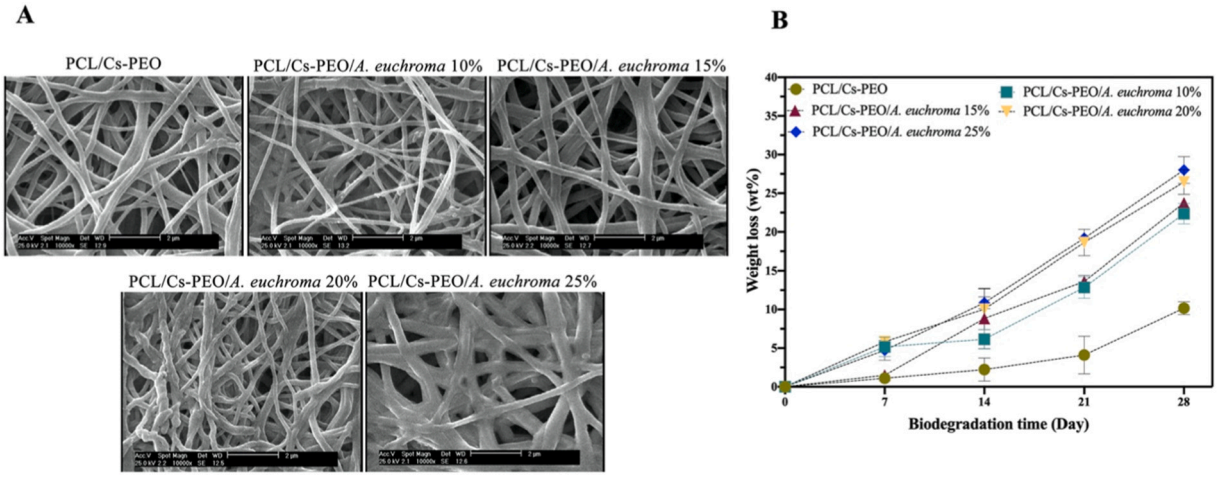

Fig. 5. SEM images of PCL/Cs-PEO and PCL/Cs-PEO/*A. euchroma* nanofibers after 24 h treatment with PBS solution (Scale bar: 2 μm) (A). Biodegradation of nanofibers scaffolds in PBS and lysozyme enzyme solution at 37 °C for 28 days. Weight loss of PCL/Cs-PEO/*A. euchroma* 25% nanofibers compared with other nanofibers was meaningfully faster (B).

water vapor molecules; therefore, the diameter of the nanofibrous scaffold increases after immersing in PBS.

3.9. Cytotoxicity assays

To study the potential of fabricated nanofibrous scaffolds for skin regeneration, cytotoxicity study was carried out by XTT assay as first step. For this aim, human dermal fibroblasts cells (HDF) were used to specify skin cell's behavior in the presence of the nanofibrous scaffolds. The dermal fibroblast is one of the primary cell types of the dermis layer of skin and plays a vital role in synthesizing collagen, elastin, and the viscous gel within the dermis (Gawkrodger & Ardern-Jones, 2016). Fig. 6A reports the cytotoxicity test results on HDF fibroblast cells seeding directly on nanofibrous scaffolds, which is based on cell metabolic activity. To remove the effect of the residual polymers and organic solvent on cellular viability, nanofibers were washed with distilled water several times. Results showed that the prepared nanofibrous scaffolds are non-toxic because their metabolic activity was higher than the control group, and also, they have positively affected on cells proliferation. The cell metabolic activity presented variations between samples. The XTT assay for HDF cells seeded on the PCL/Cs-PEO containing *A. euchroma* extract nanofibers exhibited no statistically significant differences in viability compared to each other, which confirmed similar metabolic activities in all scaffolds. But there is a significant difference in cell viability of PCL/Cs-PEO compared to nanofibers containing *A. euchroma* 20% ($*p < 0.05$), which can be explained by the positive effect on cell proliferation *A. euchroma* compared with PCL/Cs-PEO nanofibrous scaffolds without *A. euchroma*. The best cytocompatibility results are related to the nanofibrous scaffolds containing *A. euchroma* 15% and 20% (102% and 103%, respectively). This result reveals that the composition of the scaffolds is appropriate for dermis cells without production of any reactive oxygen species (ROS) (Chompoosor et al., 2010; Radwan-Pragłowska, Janus, Piątkowski, Bogdał, & Matýsek, 2020). So, the fabricated nanofibrous scaffolds can be considered safe and non-toxic thus, they can potentially be used in tissue engineering and regenerative medicine applications. The target of tissue engineering and regenerative medicine is to assist defective organs to regenerate; thus, the bioactivity and biosafety of scaffolds is a highly necessary (Radwan-Pragłowska et al., 2020; Zhao, Zhang, Lu, & Xu, 2015). Lactate dehydrogenase (LDH) assay was used to estimate scaffold biocompatibility by LDH as a substitute marker for membrane disruption in human dermal fibroblast cells. In spite of the fact that some cytotoxicity was seen over different time points, as yet even in the worst case, cytotoxicity amount has not increased than 15%, which confirms that the selected biomaterial for preparing scaffolds has a suitable potential for tissue engineering and skin regeneration application (Fig. 6B).

3.10. Cell attachment and morphology

Cell seeding and SEM studies were carried out to investigate the cell attachment and morphology on the scaffolds. Cells seeded on all scaffolds with and without the presence of *A. euchroma* extract showed proper cell adhesion and proliferating activity. As shown in the cytotoxicity assay, the toxicity level of the prepared biomaterials was considered safe. As shown in Fig. 6C, after five days of cell culture, the fibroblasts created a uniform sheet on scaffolds and interconnected with

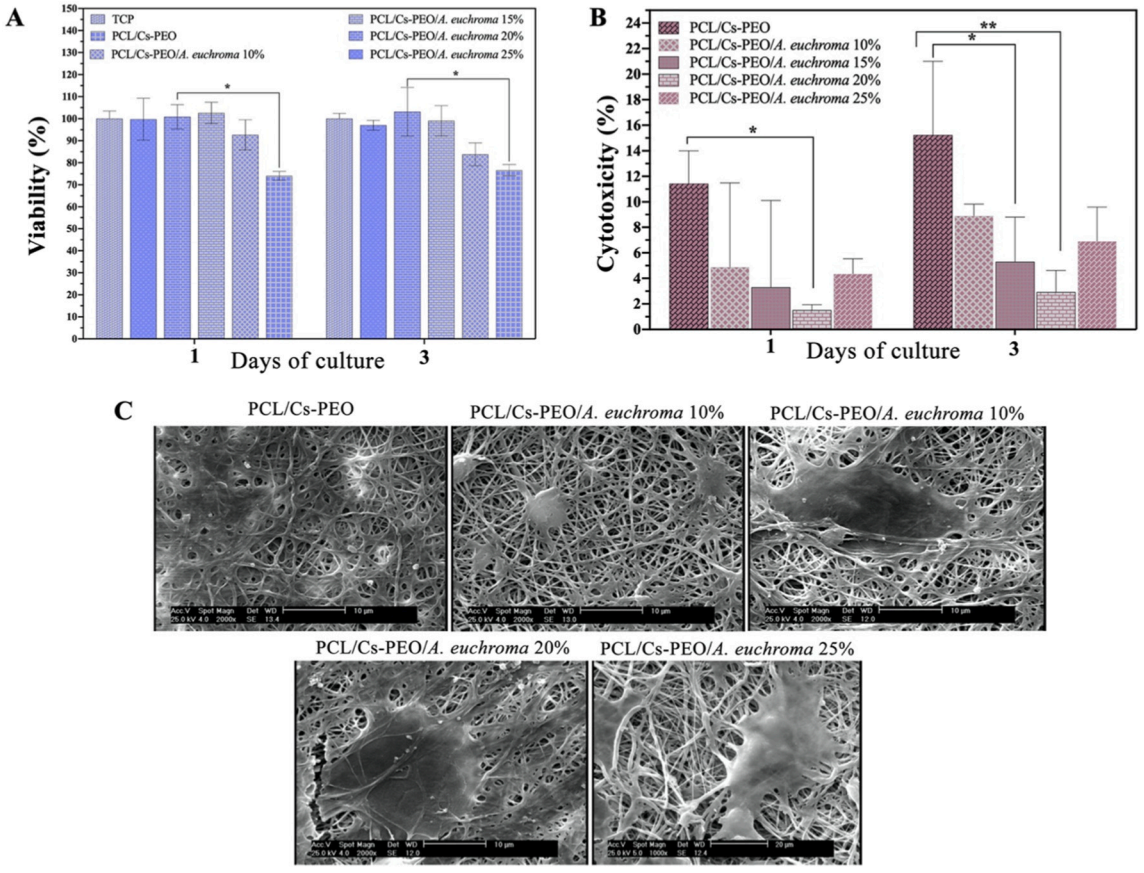

Fig. 6. In vitro cytocompatibility was assessed by the XTT assay of HDF cells seeded on PCL/Cs-PEO and *A. euchroma* loaded PCL/Cs-PEO nanofibers after 1 and 3 days of culture. No significant differences were seen using ANOVA with Tukey's multiple comparisons test between different concentration of *A. euchroma* (*compared to PCL/Cs-PEO nanofibers, $n = 6$, $*p < 0.05$, Mean ± SD). There is only a significant difference between PCL/Cs-PEO/*A. euchroma* 20% and PCL/Cs-PEO nanofibrous scaffolds (A). The LDH cytotoxicity assay on HDF cells (B). Scanning electron microscopy (SEM) images of normal Human Dermal Fibroblast (HDF) cells on the nanofibrous scaffolds at 5 days (C). All samples were compared with TCP and PCL/Cs-PEO nanofiber * is referred to $P \leq 0.0344$, ** and for $P \leq 0.0039$.

ECM. However, longer than 5 days of cellular studies may demonstrate a better vision of cellular activities. SEM micrograph images display suitable cell spreading and cell attachment on nanofibrous scaffolds with and without the presence of *A. euchroma* extract. Normal cells have a spindle, longitudinal shape, and oval nuclei. So, the size and shape of cells on nanofibrous scaffolds were similar to normal cells. This represents the highest simulation in the biological responses to the in vivo conditions. The HDF cells sheet exists and proliferates on the scaffold, and some interactions may happen between biomaterials and fibroblasts. It was demonstrated that the PCL/Cs-PEO/*A. euchroma* nanofibrous scaffolds have a suitable biocompatibility and ability to stimulate the proliferation of HDF on nanofibers. This effect should be due to the anti-inflammatory effect of *A. euchroma*. The anti-inflammatory effects of *A. euchroma* and its derivates shikonin may be related to mechanisms like inhibition of the respiratory burst in neutrophils and biosynthesis of leukotriene B4, suppression of mast cell degranulation, change of phosphatidylinositol-mediated signaling pathway, or blockade of chemokine binding to the CCR-1 (Hosseini, Mirzaee, Davoodi, Jouybari, & Azadbakht, 2018; Kourounakis, Assimopoulou, Papageorgiou, Gavalas, & Kourounakis, 2002). Moreover, Landa P et al. have reported that *A.euchroma* derivatives such as shikonin are able to have higher potency as a COX inhibitor than alkannin (Landa et al., 2012). Han et al. have reported poly(ε-caprolactone) (PCL)/poly (trimethylene carbonate) (PTMC) nanofibrous scaffolds containing shikonin for potential use in wound healing (Han, Chen, Branford-White, & Zhu, 2009). They have proposed the shikonin-loaded nanofibrous scaffolds are able to treatment of wound healing and inhibition bacterial growth. Several studies have been conducted about the pharmacological and histopathological benefits of *A.Euchroma* in the wound healing process. They have confirmed that the *A.euchroma* can improve fibroblast proliferation, collagen synthesis, angiogenesis, and degree of inflammation (Ashkani-Esfahani et al., 2012; Henry & Garner, 2003; Nasiri et al., 2016; Papageorgiou, Assimopoulou, & Ballis, 2008). Nasiri et al. have reported that the *A.euchroma* can significantly increase the cell proliferation and migration in the wound area compared to silver sulfadiazine (SSD) (Nasiri et al., 2016). Sidhu et al. reported that Arnebin-1 are able to accelerate wound healing process. They have also revealed that the levels of Transforming growth factor beta-1 (TGFß1) are increased in wound healing (Sidhu et al., 1999).

3.11. In-vitro drug release study

The release profiles of extract with the concentrations of 10%, 15%, 20% and 25% *A. euchroma* loaded electrospun PCL/Cs-PEO nanofibrous scaffolds were monitored in phosphate buffer saline, methanol, and tween 80 (pH = 7.4) by periodically measuring the absorbance of *A. euchroma* at 575 nm via UV–Vis spectroscopy. As noted before, *A. euchroma* has hydrophobic nature, and media of release must contain methanol and tween 80, which the release process is done perfectly. The release profile of the different concentrations of *A. euchroma* in release media (in triplicate) is represented in Fig. 7. As can be seen in this graph, a burst release during the first hour was viewed for all samples and reached their highest values in 5 h, then remained steady up to the end. Within the first 5 h of study, the release of *A. euchroma* 10% from nanofibers was lower than that of *A. euchroma* 25%. The *A. euchroma* 10%, 15%, 20%, and 25% loaded PCL/Cs-PEO nanofibers exhibits a burst release 11%, 23%, 28%, and 35% respectively. An initial large bolus of the drug, which can be released at the first hours is known as 'burst release' and can cause higher immediate drug delivery in the targeted area.

Moreover, burst release is one of the critical drug administration strategies which can be used for drug delivery systems with high release rates (Cam et al., 2020; Huang & Brazel, 2001; Wang, Chang, Ahmad, Zheng, & Li, 2017). As the literature mentioned, to proper wound treatment, an initial burst release of drugs can provide instant sedation, and then sustain release can improve gradual wound healing (Setterstrom, Tice, & Myers, 1984). Therefore the initial burst release of *A. euchroma* from the fabricated PCL/Cs-PEO nanofibrous scaffolds can be valuable for wound treatment application. In this regard, the initial burst release is anticipated since the hydrophilic Cs were part of composite two-layered nanofibrous scaffolds. Since PEO and Cs biopolymers possess water absorption and swelling, diffusion and polymer weakness are involved in the release mechanism. In 96 h, maximum amounts of *A. euchroma* released from nanofibers containing 10%, 15%, 20%, and 25% drug were 12%, 26%, 33%, and 41%, respectively. Kim et al. demonstrated that the burst effect of drug release from nanofibrous

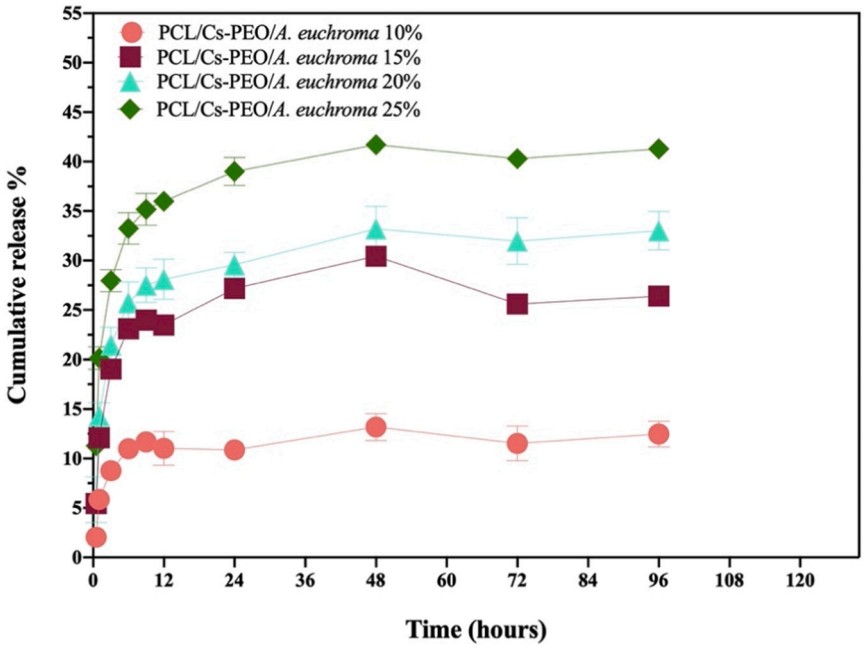

Fig. 7. In vitro release study of the *A. euchroma* from the two-layer electrospun PCL/Cs-PEO nanofibers in PBS, methanol 10%, and tween 80 (pH = 7.4) (Mean ± SD).

scaffolds was affected via fragile physical interactions between the polymer and drug. The drug molecules existed on the surface of nanofibers and were simply released when exposed to aqueous media (Kim et al., 2004). Therefore, extract with hydrophobic nature can easily place on the surface of nanofibrous scaffolds and rapidly released when exposed to aqueous media.

Moreover, the immediate and complete extract releases increased by enhancing extract concentration because more extract is located in the nanofibers' surface. The most drug release from PCL/Cs-PEO nanofibers in the optimized situation was approximately 41%. It occurred due to the trapping of drug molecules between the pores of nanofibrous scaffolds (Rambhia & Ma, 2015). From a medicinally view point, due to maximum release of two-layer nanofibrous scaffolds, it can be applied as wound dressing for more assessment at regenerative medicine and animal model.

3.12. Antibacterial activity

The antibacterial activity of nanofibrous scaffolds against *E. coli* and *S. aureus* was assessed by a dynamic contact assay and the agar plate culture method. To evaluate the dynamic contact assay, bacterial suspensions were incubated with PCL/Cs-PEO and PCL/Cs-PEO containing various concentrations of *A.euchroma* nanofibers for up to 24 h. Antibacterial results showed that the PCL/Cs-PEO, PCL/Cs-PEO/*A.euchroma* 10%, PCL/Cs-PEO/*A.euchroma* 15%, PCL/Cs-PEO/*A.euchroma* 20%, and PCL/Cs-PEO/*A.euchroma* 25% inhibited 38.7%, 57.5%, 56.6%, 32.1%, and 13.5% of *E. coli* at 24 h, respectively. As shown in Fig. 8A, there was a significant difference between PCL/Cs-PEO/*A.euchroma* 10% and PCL/Cs-PEO/*A.euchroma* 15% with PCL/Cs-PEO nanofibers in the inhibition of *E. coli* at 24 h. Moreover, the antibacterial results of nanofibers containing *A.euchroma* indicated that the inhibition of *E. coli* was not dose-dependent. Antibacterial inhibition of *S. aureus* at 24 h demonstrated that the PCL/Cs-PEO, PCL/Cs-PEO/*A.euchroma* 10%, PCL/Cs-PEO/*A.euchroma* 15%, PCL/Cs-PEO/*A.euchroma* 20%, and PCL/Cs-PEO/*A.euchroma* 25% have 17.0%, 43.2%, 42.1%, 59.5%, and 44.5% antibacterial property, respectively. The antibacterial activity and long-term bacteriostatic effect play a vital role in wound healing process. It is noteworthy that the antibacterial activity of PCL/Cs-PEO/*A.euchroma* against *S. aureus* was approximately noticeable compared with *E. coli*. It seems that the PCL/Cs-PEO/*A.euchroma* nanofibrous scaffold may be beneficial to wound treatment. SEM analysis was performed to evaluate the antibacterial activity of the nanofibrous scaffolds (Fig. 8B). After treatment with nanofibrous scaffold, the morphology of bacteria was changed with some dents and dimple, and also the structure of bacteria has been destroyed. In the case of PCL/Cs-PEO and PCL/Cs-PEO/*A. euchroma* 25% of the bacteria had intact morphology, while the total number of bacteria on PCL/Cs-PEO/*A.euchroma* 15% and PCL/Cs-PEO/*A.euchroma* 20% had remarkably decreased.

4. Conclusions

The present study showed that hybrid nanofibrous scaffolds based on PCL and chitosan-PEO polymer fabricated by two-nozzle electrospinning could improve skin regeneration and wound healing. Further

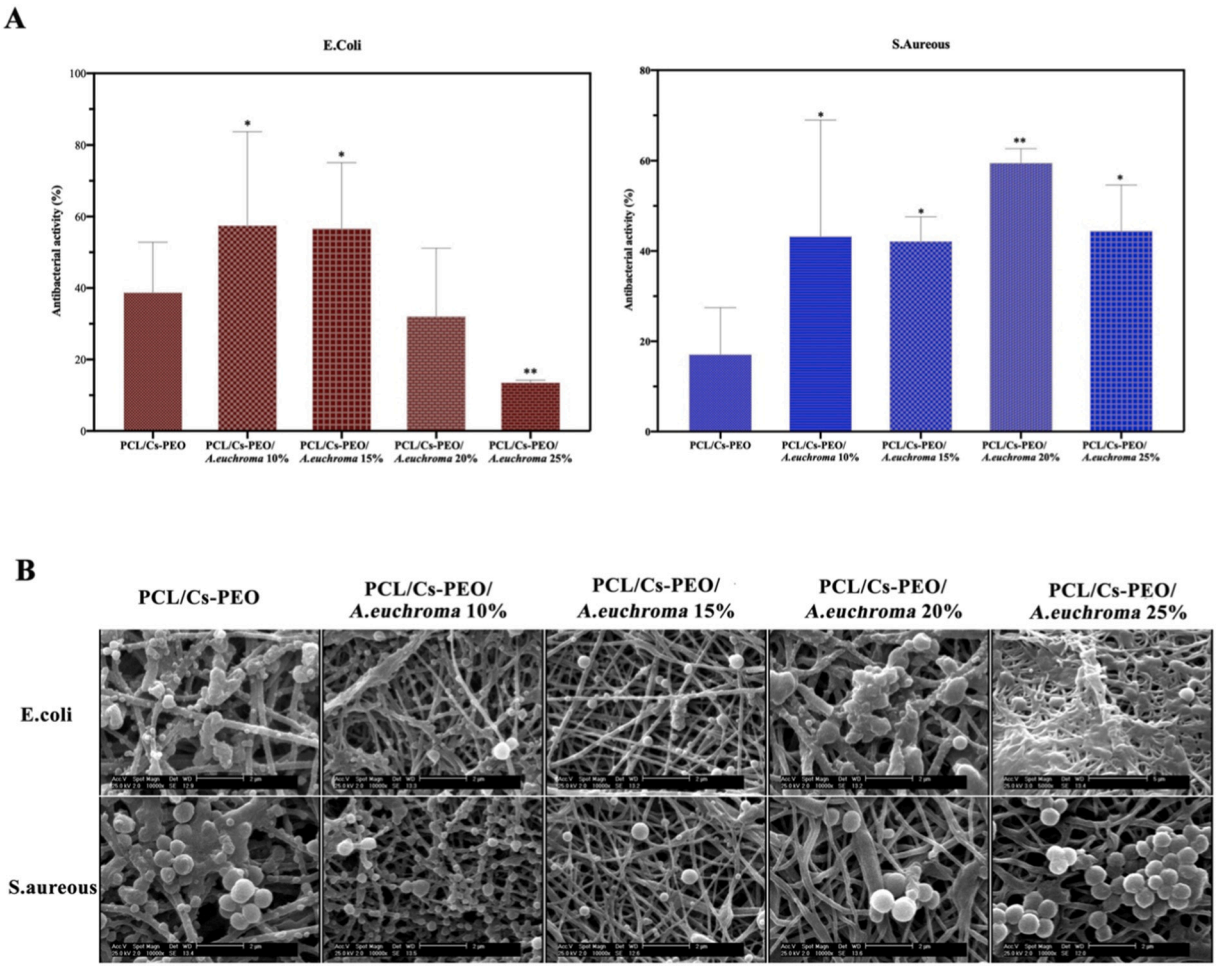

Fig. 8. Antibacterial activity of PCL/Cs-PEO and PCL/Cs-PEO/*A.euchroma* nanofibers with dynamic contact assay after 24 h (A). SEM images of morphological characterization of bacteria on PCL/Cs-PEO and PCL/Cs-PEO/*A. euchroma* nanofibers after 24 h (B).

assessment of their mechanical strength, capability to biodegradation, and drug release profile confirm that these biomaterials possess the potential of these skin tissue scaffolds to increase the wound healing process. In particular, the antibacterial activities of the *A.euchroma*-loaded nanofibrous scaffolds were evaluated, which demonstrated that the PCL/Cs-PEO/*A.euchroma* nanofibrous scaffolds possess good performance against bacteria. Finally, cytotoxicity and bioactivity test on human dermal fibroblast cells have demonstrated the cytocompatibility of the hybrid scaffolds. Moreover, it was shown that incorporating *A. euchroma* into polymeric nanofibrous scaffolds improved cell proliferation and cell attachment on nanofibrous scaffolds. Thus, the proposed composition exhibits promising properties for the aimed tissue engineering application, particularly in the case of skin burns. We believe that studying more sophisticated cellular assessments and vascularization potential for thick wound treatments would open new windows for revolutionizing skin tissue engineering. Moreover, the fabricated nanofibrous scaffolds may be used in a patch shape onto the site of a burn wound in the future. However, in vivo studies must be performed to obtain more information about the possible use in the clinical trial. In a long run, the fabricated PCL/Cs-PEO/*A.euchroma* will be evaluated based on the animal model to reveal its clinical availability. However, the fabricated hybrid nanofibrous scaffold of considerable cytocompatibility, mechanical strength and bactericidal activity in our present study may be promising potential as wound dressings and drug delivery carriers for wound healing in the future.

CRediT authorship contribution statement

Fatemeh Asghari: Conceptualization, Methodology, Writing – original draft. **Davood Rabiei Faradonbeh:** Methodology, Software. **Ziba Veisi Malekshahi:** Writing – original draft, Investigation. **Houra Nekounam:** Writing – original draft, Investigation. **Behnaz Ghaemi:** Writing – review & editing. **Yaser Yousefpoor:** Methodology. **Hossein Ghanbari:** Supervision. **Reza Faridi-Majidi:** Writing – review & editing, Supervision.

Acknowledgment

This research was funded by Tehran University of Medical Sciences and Health Services (TUMS), grant no 97-03-87-41008.

References

Abid, S., Hussain, T., Nazir, A., Zahir, A., Ramakrishna, S., Hameed, M., & Khenoussi, N. (2019). Enhanced antibacterial activity of PEO-chitosan nanofibers with potential application in burn infection management. *International Journal of Biological Macromolecules, 135*, 1222–1236.

Akbarinejad, A., Ghoorchian, A., Kamalabadi, M., & Alizadeh, N. (2016). Electrospun soluble conductive polypyrrole nanoparticles for fabrication of highly selective n-butylamine gas sensor. *Sensors and Actuators B: Chemical, 236*, 99–108.

Asghari, F., Ghanbari, H., Moghimi, H. R., Takzaree, N., Nekounam, H., & Faridi-Majidi, R. (2021). *Study on the chemistry identification and assessment of antioxidant and antibacterial activity of the biologically active constituents from the roots of Arnebia euchroma for promising application in nanomedicine and pharmaceutical*.

Ashkani-Esfahani, S., Imanieh, M. H., Khoshneviszadeh, M., Meshksar, A., Noorafshan, A., Geramizadeh, B., Ebrahimi, S., Handjani, F., & Tanideh, N. (2012). The healing effect of arnebia euchroma in second degree burn wounds in rat as an animal model. *Iranian Red Crescent Medical Journal, 14*(2), 70.

Atiyeh, B. S., Ioannovich, J., Al-Amm, C. A., & El-Musa, K. A. (2002). Management of acute and chronic open wounds: The importance of moist environment in optimal wound healing. *Current Pharmaceutical Biotechnology, 3*(3), 179–195.

Barnes, C. P., Sell, S. A., Boland, E. D., Simpson, D. G., & Bowlin, G. L. (2007). Nanofiber technology: Designing the next generation of tissue engineering scaffolds. *Advanced Drug Delivery Reviews, 59*(14), 1413–1433.

Boateng, J. S., Matthews, K. H., Stevens, H. N. E., & Eccleston, G. M. (2008). Wound healing dressings and drug delivery systems: A review. *Journal of Pharmaceutical Sciences, 97*(8), 2892–2923.

Budovsky, A., Yarmolinsky, L., & Ben-Shabat, S. (2015). Effect of medicinal plants on wound healing. *Wound Repair and Regeneration, 23*(2), 171–183.

Cam, M. E., Yildiz, S., Alenezi, H., Cesur, S., Ozcan, G. S., Erdemir, G., Edirisinghe, U., Akakin, D., Kuruca, D. S., & Kabasakal, L. (2020). Evaluation of burst release and sustained release of pioglitazone-loaded fibrous mats on diabetic wound healing: An in vitro and in vivo comparison study. *Journal of the Royal Society Interface, 17*(162), 20190712.

Cao, H., Zhang, W., Liu, D., Hou, M., Liu, S., He, W., Lin, J., & Shao, M. (2020). Identification, in vitro evaluation and modeling studies of the constituents from the roots of Arnebia euchroma for antitumor activity and STAT3 inhibition. *Bioorganic Chemistry*. https://doi.org/10.1016/j.bioorg.2020.103655

Chanda, A., Adhikari, J., Ghosh, A., Chowdhury, S. R., Thomas, S., Datta, P., & Saha, P. (2018). Electrospun chitosan/polycaprolactone-hyaluronic acid bilayered scaffold for potential wound healing applications. *International Journal of Biological Macromolecules, 116*, 774–785.

Chen, Q., Tu Fan, J., Sarkar, M. K., & Bal, K. (2011). Plant-based biomimetic branching structures in knitted fabrics for improved comfort-related properties. *Textile Research Journal, 81*(10), 1039–1048.

Chompoosor, A., Saha, K., Ghosh, P. S., Macarthy, D. J., Miranda, O. R., Zhu, Z., Arcaro, K. F., & Rotello, V. M. (2010). The role of surface functionality on acute cytotoxicity, ROS generation and DNA damage by cationic gold nanoparticles. *Small, 6*(20), 2246–2249.

Cipitria, A., Skelton, A., Dargaville, T. R., Dalton, P. D., & Hutmacher, D. W. (2011). Design, fabrication and characterization of PCL electrospun scaffolds—A review. *Journal of Materials Chemistry, 21*(26), 9419–9453.

Dawson, E., Mapili, G., Erickson, K., Taqvi, S., & Roy, K. (2008). Biomaterials for stem cell differentiation. *Advanced Drug Delivery Reviews, 60*(2), 215–228.

Devlin, J. J., Kircher, S., Kozen, B. G., Littlejohn, L. F., & Johnson, A. S. (2011). Comparison of ChitoFlex®, CELOXTM, and QuikClot® in control of hemorrhage. *The Journal of Emergency Medicine, 41*(3), 237–245. https://doi.org/10.1016/j.jemermed.2009.02.017

Dhivya, S., Padma, V. V., & Santhini, E. (2015). Wound dressings–a review. *Biomedicine, 5*(4).

Feng, Y., Xiong, T., Jiang, S., Liu, S., & Hou, H. (2016). Mechanical properties and chemical resistance of electrospun polyterafluoroethylene fibres. *RSC Advances, 6*(29), 24250–24256.

Fernandes Queiroz, M., Melo, K. R. T., Sabry, D. A., Sassaki, G. L., & Rocha, H. A. O. (2015). Does the use of chitosan contribute to oxalate kidney stone formation? *Marine Drugs, 13*(1), 141–158.

Gao, C., Zhang, L., Wang, J., Jin, M., Tang, Q., Chen, Z., Cheng, Y., Yang, R., & Zhao, G. (2021). Electrospun nanofibers promote wound healing: Theories, techniques, and perspectives. *Journal of Materials Chemistry B, 9*(14), 3106–3130.

Gawkrodger, D., & Ardern-Jones, M. R. (2016). Dermatology e-book: An illustrated colour text. *Elsevier Health Sciences*.

Ghasemi-Mobarakeh, L., Prabhakaran, M. P., Tian, L., Shamirzaei-Jeshvaghani, E., Dehghani, L., & Ramakrishna, S. (2015). Structural properties of scaffolds: Crucial parameters towards stem cells differentiation. *World Journal of Stem Cells, 7*(4), 728.

Gittens, R. A., Scheideler, L., Rupp, F., Hyzy, S. L., Geis-Gerstorfer, J., Schwartz, Z., & Boyan, B. D. (2014). A review on the wettability of dental implant surfaces II: Biological and clinical aspects. *Acta Biomaterialia, 10*(7), 2907–2918.

Goonoo, N., & Bhaw-Luximon, A. (2020). Nanomaterials combination for wound healing and skin regeneration. In *Advanced 3D-printed systems and nanosystems for drug delivery and tissue engineering* (pp. 159–217). Elsevier.

Goonoo, N., Bhaw-Luximon, A., Jonas, U., Jhurry, D., & Schönherr, H. (2017). Enhanced differentiation of human preosteoblasts on electrospun blend fiber mats of polydioxanone and anionic sulfated polysaccharides. *ACS Biomaterials Science & Engineering, 3*(12), 3447–3458.

Goonoo, N., Bhaw-Luximon, A., Passanha, P., Esteves, S., Schönherr, H., & Jhurry, D. (2017). Biomineralization potential and cellular response of PHB and PHBV blends with natural anionic polysaccharides. *Materials Science and Engineering: C, 76*, 13–24.

Han, J., Chen, T.-X., Branford-White, C. J., & Zhu, L.-M. (2009). Electrospun shikonin-loaded PCL/PTMC composite fiber mats with potential biomedical applications. *International Journal of Pharmaceutics, 382*(1), 215–221. https://doi.org/10.1016/j.ijpharm.2009.07.027

Han, J., Zhang, H.-T., Zhu, L.-M., & Branford-White, C. (2009). Electrospun biodegradable nanofiber mats for controlled release of herbal medicine. In *2009 3rd International Conference on Bioinformatics and Biomedical Engineering* (pp. 1–4).

He, J., Liang, Y., Shi, M., & Guo, B. (2020). Anti-oxidant electroactive and antibacterial nanofibrous wound dressings based on poly (ε-caprolactone)/quaternized chitosan-graft-polyaniline for full-thickness skin wound healing. *Chemical Engineering Journal, 385*, Article 123464.

Henry, G., & Garner, W. L. (2003). Inflammatory mediators in wound healing. *Surgical Clinics, 83*(3), 483–507.

Hiep, N. T., & Lee, B.-T. (2010). Electro-spinning of PLGA/PCL blends for tissue engineering and their biocompatibility. *Journal of Materials Science: Materials in Medicine, 21*(6), 1969–1978.

Hild, M., Al Rez, M. F., Aibibu, D., Toskas, G., Cheng, T., Laourine, E., & Cherif, C. (2015). Pcl/chitosan blended nanofibrous tubes made by dual syringe electrospinning. *Autex Research Journal, 15*(1), 54–59.

Hosseini, A., Mirzaee, F., Davoodi, A., Jouybari, H. B., & Azadbakht, M. (2018). The traditional medicine aspects, biological activity and phytochemistry of arnebia spp. *Medicinski Glasnik, 15*(1).

Huang, X., & Brazel, C. S. (2001). On the importance and mechanisms of burst release in matrix-controlled drug delivery systems. *Journal of Controlled Release, 73*(2–3), 121–136.

Islam, M. M., Shahruzzaman, M., Biswas, S., Sakib, M. N., & Rashid, T. U. (2020). Chitosan based bioactive materials in tissue engineering applications-a review. *Bioactive Materials, 5*(1), 164–183.

Janarthanan, G., & Noh, I. (2021). *Overview of injectable hydrogels for 3D bioprinting and tissue regeneration*.

Ketabchi, N., Dinarvand, R., Adabi, M., Gholami, M., Firoozi, S., Amanzadi, B., & Faridi-Majidi, R. (2020). *Study of third-degree burn wounds debridement and treatment by actinidin enzyme immobilized on electrospun chitosan/PEO nanofibers in rats*.

Kim, K., Luu, Y. K., Chang, C., Fang, D., Hsiao, B. S., Chu, B., & Hadjiargyrou, M. (2004). Incorporation and controlled release of a hydrophilic antibiotic using poly (lactide-co-glycolide)-based electrospun nanofibrous scaffolds. *Journal of Controlled Release, 98*(1), 47–56.

Kohane, D. S., & Langer, R. (2008). Polymeric biomaterials in tissue engineering. *Pediatric Research, 63*(5), 487–491.

Kourounakis, A. P., Assimopoulou, A. N., Papageorgiou, V. P., Gavalas, A., & Kourounakis, P. N. (2002). Alkannin and shikonin: Effect on free radical processes and on inflammation-a preliminary pharmacochemical investigation. *Archiv Der Pharmazie: An International Journal Pharmaceutical and Medicinal Chemistry, 335*(6), 262–266.

Kumar, A., Shashni, S., Kumar, P., Pant, D., Singh, A., & Verma, R. K. (2021). Phytochemical constituents, distributions and traditional usages of arnebia euchroma: A review. *Journal of Ethnopharmacology, 113896*.

Landa, P., Kutil, Z., Temml, V., Vuorinen, A., Malik, J., Dvorakova, M., Marsik, P., Kokoska, L., Pribylova, M., & Schuster, D. (2012). Redox and non-redox mechanism of in vitro cyclooxygenase inhibition by natural quinones. *Planta Medica, 78*(04), 326–333.

Lee, J., Tae, G., Kim, Y. H., Park, I. S., Kim, S.-H., & Kim, S. H. (2008). The effect of gelatin incorporation into electrospun poly (l-lactide-co-ε-caprolactone) fibers on mechanical properties and cytocompatibility. *Biomaterials, 29*(12), 1872–1879.

Lei, J., Sun, L., Li, P., Zhu, C., Lin, Z., Mackey, V., Coy, D. H., & He, Q. (2019). The wound dressings and their applications in wound healing and management. *Health Science Journal, 13*(4), 1–8.

Liu, Y., Ma, L., & Gao, C. (2012). Facile fabrication of the glutaraldehyde cross-linked collagen/chitosan porous scaffold for skin tissue engineering. *Materials Science and Engineering: C, 32*(8), 2361–2366.

Loh, Q. L., & Choong, C. (2013). Three-dimensional scaffolds for tissue engineering applications: Role of porosity and pore size. *Tissue Engineering Part B: Reviews, 19*(6), 485–502.

Lou, C.-W., Wu, Z.-H., Lee, M.-C., Chen, Y.-S., & Lin, J.-H. (2017). Polyvinyl alcohol/ lithospermum erythrorhizon nanofibrous membrane: characterizations, in vitro drug release, and cell viability. *Applied Sciences, 7*(11). https://doi.org/10.3390/app7111143

Lu, H.-T., Jiang, Y., & Chen, F. (2004). Preparative high-speed counter-current chromatography for purification of shikonin from the Chinese medicinal plant Lithospermum erythrorhizon. *Journal of Chromatography A, 1023*(1), 159–163.

Lu, T., Li, Y., & Chen, T. (2013). Techniques for fabrication and construction of three-dimensional scaffolds for tissue engineering. *International Journal of Nanomedicine, 8*, 337.

Madni, A., Kousar, R., Naeem, N., & Wahid, F. (2021). Recent advancements in applications of chitosan-based biomaterials for skin tissue engineering. *Journal of Bioresources and Bioproducts, 6*(1), 11–25. https://doi.org/10.1016/j.jobab.2021.01.002

Mohamed, M. A., Jaafar, J., Ismail, A. F., Othman, M. H. D., & Rahman, M. A. (2017). Fourier transform infrared (FTIR) spectroscopy. In *Membrane characterization* (pp. 3–29). Elsevier.

Nasiri, E., Hosseinimehr, S. J., Zaghi Hosseinzadeh, A., Azadbakht, M., Akbari, J., & Azadbakht, M. (2016). The effects of arnebia euchroma ointment on second-degree burn wounds: A randomized clinical trial. *Journal of Ethnopharmacology, 189*, 107–116. https://doi.org/10.1016/j.jep.2016.05.029

Okur, M. E., Karantas, I. D., Şenyiğit, Z., Üstündağ Okur, N., & Siafaka, P. I. (2020). Recent trends on wound management: New therapeutic choices based on polymeric carriers. *Asian Journal of Pharmaceutical Sciences, 15*(6), 661–684. https://doi.org/10.1016/j.ajps.2019.11.008

Pakravan, M., Heuzey, M.-C., & Ajji, A. (2011). A fundamental study of chitosan/PEO electrospinning. *Polymer, 52*(21), 4813–4824.

Papageorgiou, V., Assimopoulou, A., & Ballis, A. (2008). Alkannins and shikonins: A new class of wound healing agents. *Current Medicinal Chemistry*. https://doi.org/10.2174/092986708786848532

Papageorgiou, V. P., Assimopoulou, A. N., Couladouros, E. A., Hepworth, D., & Nicolaou, K. C. (1999). The chemistry and biology of alkannin, shikonin, and related naphthazarin natural products. *Angewandte Chemie - International Edition*. https://doi.org/10.1002/(SICI)1521-3773(19990201)38:3<270::AID-ANIE270>3.0.CO;2-0

Prasad, T., Shabeena, E. A., Vinod, D., Kumary, T. V., & Kumar, P. R. A. (2015). Characterization and in vitro evaluation of electrospun chitosan/polycaprolactone blend fibrous mat for skin tissue engineering. *Journal of Materials Science: Materials in Medicine, 26*(1), 28.

Qian, Y., Zhang, Z., Zheng, L., Song, R., & Zhao, Y. (2014). *Fabrication and characterization of electrospun polycaprolactone blended with chitosan-gelatin complex nanofibrous mats. 2014*.

Radwan-Pragłowska, J., Janus, Ł., Piątkowski, M., Bogdał, D., & Matýsek, D. (2020). Hybrid bilayer PLA/chitosan nanofibrous scaffolds doped with ZnO, Fe3O4, and au nanoparticles with bioactive properties for skin tissue engineering. *Polymers, 12*(1), 159.

Rahaman, M. N., Day, D. E., Bal, B. S., Fu, Q., Jung, S. B., Bonewald, L. F., & Tomsia, A. P. (2011). Bioactive glass in tissue engineering. *Acta Biomaterialia, 7*(6), 2355–2373.

Ramalingam, M., & Ramakrishna, S. (2017). Introduction to nanofiber composites. In *Nanofiber Composites for Biomedical Applications* (pp. 3–29). Elsevier.

Rambhia, K. J., & Ma, P. X. (2015). Controlled drug release for tissue engineering. *Journal of Controlled Release, 219*, 119–128.

Rezvani Ghomi, E., Khalili, S., Nouri Khorasani, S., Esmaeely Neisiany, R., & Ramakrishna, S. (2019). Wound dressings: Current advances and future directions. *Journal of Applied Polymer Science, 136*(27), 47738.

Sell, S., Barnes, C., Smith, M., McClure, M., Madurantakam, P., Grant, J., Mcmanus, M., & Bowlin, G. (2007). Extracellular matrix regenerated: Tissue engineering via electrospun biomimetic nanofibers. *Polymer International, 56*(11), 1349–1360.

Setterstrom, J. A., Tice, T. R., & Myers, W. E. (1984). *Recent advances in drug delivery systems*.

Shalumon, K. T., Anulekha, K. H., Chennazhi, K. P., Tamura, H., Nair, S. V., & Jayakumar, R. (2011). Fabrication of chitosan/poly (caprolactone) nanofibrous scaffold for bone and skin tissue engineering. *International Journal of Biological Macromolecules, 48*(4), 571–576.

Sidhu, G. S., Singh, A. K., Banaudha, K. K., Gaddipati, J. P., Patnaik, G. K., & Maheshwari, R. K. (1999). Arnebin-1 accelerates normal and hydrocortisone-induced impaired wound healing. *Journal of Investigative Dermatology, 113*(5), 773–781.

Sionkowska, A. (2003). Interaction of collagen and poly (vinyl pyrrolidone) in blends. *European Polymer Journal, 39*(11), 2135–2140.

Song, C., Yu, H., Zhang, M., Yang, Y., & Zhang, G. (2013). Physicochemical properties and antioxidant activity of chitosan from the blowfly Chrysomya megacephala larvae. *International Journal of Biological Macromolecules, 60*, 347–354.

Sonseca, Á., Camarero-Espinosa, S., Peponi, L., Weder, C., Foster, E. J., Kenny, J. M., & Giménez, E. (2014). Mechanical and shape-memory properties of poly (mannitol sebacate)/cellulose nanocrystal nanocomposites. *Journal of Polymer Science Part A: Polymer Chemistry, 52*(21), 3123–3133.

Svensjö, T., Pomahac, B., Yao, F., Slama, J., & Eriksson, E. (2000). Accelerated healing of full-thickness skin wounds in a wet environment. *Plastic and Reconstructive Surgery, 106*(3), 602–612.

Taepaiboon, P., Rungsardthong, U., & Supaphol, P. (2007). Vitamin-loaded electrospun cellulose acetate nanofiber mats as transdermal and dermal therapeutic agents of vitamin A acid and vitamin E. *European Journal of Pharmaceutics and Biopharmaceutics, 67*(2), 387–397.

Takagi, N., Kawakami, K., Kanno, E., Tanno, H., Takeda, A., Ishii, K., Imai, Y., Iwakura, Y., & Tachi, M. (2017). IL-17A promotes neutrophilic inflammation and disturbs acute wound healing in skin. *Experimental Dermatology, 26*(2), 137–144.

Trinca, R. B., Westin, C. B., da Silva, J. A. F., & Moraes, Â. M. (2017). Electrospun multilayer chitosan scaffolds as potential wound dressings for skin lesions. *European Polymer Journal, 88*, 161–170.

Truong, A.-T. N., Kowal-Vern, A., Latenser, B. A., Wiley, D. E., & Walter, R. J. (2005). Comparison of dermal substitutes in wound healing utilizing a nude mouse model. e4–e4 *Journal of Burns and Wounds, 4* https://pubmed.ncbi.nlm.nih.gov/16921409.

Vijayakumar, V., Samal, S. K., Mohanty, S., & Nayak, S. K. (2019). Recent advancements in biopolymer and metal nanoparticle-based materials in diabetic wound healing management. *International Journal of Biological Macromolecules, 122*, 137–148.

Vino, A. B., Ramasamy, P., Shanmugam, V., & Shanmugam, A. (2012). Extraction, characterization and in vitro antioxidative potential of chitosan and sulfated chitosan from cuttlebone of Sepia aculeata orbigny, 1848. *Asian Pacific Journal of Tropical Biomedicine, 2*(1), S334–S341.

Wang, D., Cheng, W., Wang, Q., Zang, J., Zhang, Y., & Han, G. (2019). Preparation of electrospun chitosan/poly (ethylene oxide) composite nanofibers reinforced with cellulose nanocrystals: Structure, morphology, and mechanical behavior. *Composites Science and Technology, 182*, Article 107774.

Wang, D., Cheng, W., Yue, Y., Xuan, L., Ni, X., & Han, G. (2018). Electrospun cellulose nanocrystals/chitosan/polyvinyl alcohol nanofibrous films and their exploration to metal ions adsorption. *Polymers, 10*(10), 1046.

Wang, L., Chang, M.-W., Ahmad, Z., Zheng, H., & Li, J.-S. (2017). Mass and controlled fabrication of aligned PVP fibers for matrix type antibiotic drug delivery systems. *Chemical Engineering Journal, 307*, 661–669.

Wei, C., Feng, Y., Che, D., Zhang, J., Zhou, X., Shi, Y., & Wang, L. (2021). Biomaterials in skin tissue engineering. *International Journal of Polymeric Materials and Polymeric Biomaterials*, 1–19.

Wilgus, T. A., Roy, S., & McDaniel, J. C. (2013). Neutrophils and wound repair: Positive actions and negative reactions. *Advances in Wound Care, 2*(7), 379–388.

Winter, G. D. (1962). Formation of the scab and the rate of epithelization of superficial wounds in the skin of the young domestic pig. *Nature, 193*(4812), 293–294.

Xu, F., Wang, P., Zhang, X., Hou, T., Qu, L., Wang, C., Wang, J., Liu, Y., & Liang, X. (2021). Identification and target-pathway deconvolution of FFA4 agonists with anti-diabetic activity from arnebia euchroma (Royle) Johnst. *Pharmacological Research, 163*, Article 105173.

Xu, R., Xia, H., He, W., Li, Z., Zhao, J., Liu, B., Wang, Y., Lei, Q., Kong, Y., & Bai, Y. (2016). Controlled water vapor transmission rate promotes wound-healing via wound re-epithelialization and contraction enhancement. *Scientific Reports, 6*(1), 1–12.

Yin, J., & Xu, L. (2020). Batch preparation of electrospun polycaprolactone/chitosan/aloe vera blended nanofiber membranes for novel wound dressing. *International Journal of Biological Macromolecules, 160*, 352–363.

Zhao, G., Zhang, X., Lu, T. J., & Xu, F. (2015). Recent advances in electrospun nanofibrous scaffolds for cardiac tissue engineering. *Advanced Functional Materials, 25*(36), 5726–5738.

Zhishu, H., Min, Z., Lin, M., & Lianquan, G. (2000). A survey of chemical and pharmacologic studies on zicao (Arnebia sp., Lithospermum sp., and Onosma sp.). *Natural Product Research and Development, 12*(1), 73–82.

Zhong, S. P., Zhang, Y. Z., & Lim, C. T. (2010). Tissue scaffolds for skin wound healing and dermal reconstruction. *Wiley Interdisciplinary Reviews: Nanomedicine and Nanobiotechnology, 2*(5), 510–525.

Zhong, S., Teo, W. E., Zhu, X., Beuerman, R. W., Ramakrishna, S., & Yung, L. Y. L. (2006). An aligned nanofibrous collagen scaffold by electrospinning and its effects on in vitro fibroblast culture. *Journal of Biomedical Materials Research Part A: An Official Journal of The Society for Biomaterials, The Japanese Society for Biomaterials, and The Australian Society for Biomaterials and the Korean Society for Biomaterials, 79*(3), 456–463.

Zhou, L., Cai, L., Ruan, H., Zhang, L., Wang, J., Jiang, H., Wu, Y., Feng, S., & Chen, J. (2021). Electrospun chitosan oligosaccharide/polycaprolactone nanofibers loaded with wound-healing compounds of rutin and quercetin as antibacterial dressings. *International Journal of Biological Macromolecules, 183*, 1145–1154.

Zhou, W., Feng, Y., Yang, J., Fan, J., Lv, J., Zhang, L., Guo, J., Ren, X., & Zhang, W. (2015). Electrospun scaffolds of silk fibroin and poly (lactide-co-glycolide) for endothelial cell growth. *Journal of Materials Science: Materials in Medicine, 26*(1), 56.